Parametric Aerodynamic Shape Optimization Framework for Fixed Wing Applications Using Open-Source Tools

Bugra Batan[1,2*], Saleh Abuhanieh[1], Tamer Calisir[2], Sahin Yigit[1]

***Abstract*— The carbon footprint of airplanes is rising due to the increment of number of flights in the ever-growing aviation industry. Improving the aerodynamic performance of aircrafts has become a critical necessity. For this reason, aerodynamic shape optimization (ASO) is of great importance when designing the aircraft components. In this study, a computational fluid dynamics (CFD) based parametric ASO framework is designed by using open-source tools to optimize the shape of a fixed wing of aircraft in the transonic regime. The obtained results using the presented ASO framework are promising, the lift to drag ratio of a fixed wing (ONERA M6) has been relatively improved by 17.92 %.**

***Keywords*—Gradient-free optimization, Genetic Algorithm, Parametric Modelling, ONERA M6, OpenFOAM. DAKOTA**

I. Introduction

The classical Tube-And-Wing (TAW) configuration has been used for many years in civil aviation and has reached an optimum state within its limits [1]. Fuel consumption by aircrafts has been decreased since last two decades thanks to the progressive development in science and technology. [2]. But there are still long-term challenges in aerodynamic performance, flight safety and environmental sustainability in aviation industry. Due to the constantly increasing number of flights, environmental problems have started to be more obvious and its impact will be probably increase. One of the the biggest challenge of the aviation community is to reduce the environmental burden of aviation [3]. With the fast paced development of the aviation industries, the future of commercial flights is leading towards the option of travelling at low supersonic and even supersonic speeds. However, it is not a sustainable way of travel for the future because of the increase in consumption of energy required to achieve flight at such speeds. Therefore, new generation aircrafts should consist of more environmentally friendly and sustainable systems.

Manuscript received Jan. 30, 2023.
*Bugra BATAN, Turkish Aerospace, 06980 Kahramankazan, Ankara, Turkey
[1]Turkish Aerospace, Department of Computational Fluid Mechanics, Ankara, 06980, Turkey
[2]Gazi University, Graduate School of Applied and Natural Sciences, Department of Mechanical Engineering, Ankara, 06570, Turkey

Many countries and aviation authorities have recognized the crucial plight and updated their regulations on aircraft noise and emissions stricter [4]. It might be hard to satisfy these regulations without revolutionary change in the aircraft design concepts.

To start a new era based on green aviation 15 years ago, leading aviation organizations such as National Aeronautics and Space Administration (NASA) in USA and Advisory Council of Aeronautics Research in Europe (ACARE) have started to research programs respectively, Environmentally Responsible Aviation (ERA) and Clean Sky I/II [5], [6]. In these research programs, they aimed to create a new aircraft configuration that would be minimally harmful to the environment, as desired in the new strict regulations, while at the same time flying at higher cruising speeds and longer ranges. There is no single technology to offer solutions that covers whole concepts of green aviation. Existing problems can be solved by hard research in various fields such as aerodynamics, engines and aircraft systems. This can only be done by using multidisciplinary design optimization (MDO) approach to increase design efficiency of new aircraft configurations. The basis of all these researches is to increase the useful load carrying capacity of an aircraft to longer distances by using the least fuel [7], [8]. Moreover, multidisciplinary analysis and optimization are among the most prominent topics in the CFD Vision 2030 [9]. At this point, coupling CFD with ASO improves designs significantly. In the literature, there are important studies on reducing the drag coefficient in the transonic regime using ASO [10]-[14].

However, these studies [10]-[14] used commercial CFD based ASO tools which have high licence costs and do not allow users for development. Therefore, the main purpose of the study, is to offer an open-source CFD based parametric aerodynamic shape optimization workflow for high fidelity fixed wing shape optimization applications. Accordingly, the main objectives of the current study are:

i. To create an open-source based ASO workflow without the need for any license.
ii. Explain each step in the optimization cycle and how each components of the cycle works.

https://doi.org/10.17758/URUAE20.AE0323109

II. METHODOLOGY

Fig. 1. represents the workflow of the optimization cycle used in the present work which comprises 4 steps. The first step of the cycle is to create a parametric model and surface mesh related to the aircraft geometry with using OpenVSP [15]. The next step is to generate volume mesh using SUMO (SUrface MOdeler) [16] and TetGen (Tetrahedral Mesh Generator) [17].

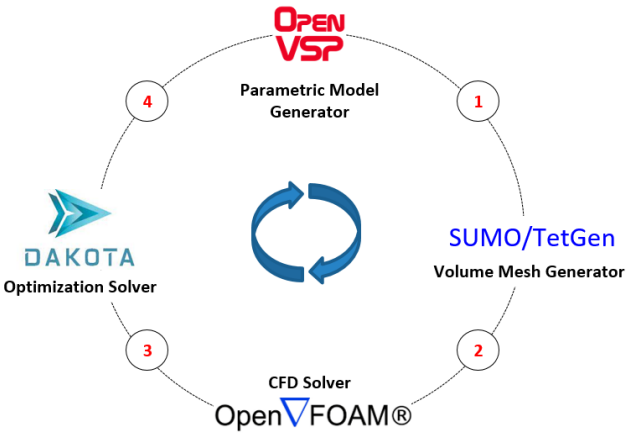

Fig. 1. Optimization workflow

At this stage, the volume mesh is ready for the chosen parametric geometry, so in the 3rd step, external flow analyzes are performed using open-source CFD solver OpenFOAM [18]. In the last step, the results obtained from the external flow analyses are sent to the optimization tool DAKOTA [19] and the new shape parameters for the next cycle step are calculated according to the determined object function and optimization algorithm. This cycle continues until the stopping criteria is achieved. In the present study, the lift-to-drag ratio for the fixed wing has been selected as the object function. In addition, the CFD solution for the wing geometry is done iteratively every cycle. ONERA M6 wing case 2308 [20] has been used as a test case due to the availability of the experimental data and many numerical results in the literature [21]. The properties of the wing are given in Table I. Drag and lift coefficient values obtained from the present work are compared with the numerical results in [21] which can be seen in Table II.

TABLE I : PROPERTIES OF ONERA M6 WING

Properties	Values
Root Chord (m)	1.0
Taper ratio	0.562
Aspect Ratio	1.90
Span (m)	2.969
Area (m²)	2.319

A. *Step-1 (Creating Parametric Model and Surface Mesh of using OpenVSP)*

With the open source based OpenVSP, any wing can be easily designed using airfoil profile and independent 3 design parameters. First of all, the wing profile has been created using the airfoil known as the ONERA D airfoil profile, and the parametric model has been created by entering other section planform parameters (aspect ratio, taper ratio and span) in the literature. The parametric model of ONERA M6 wing is given in Fig. 2.

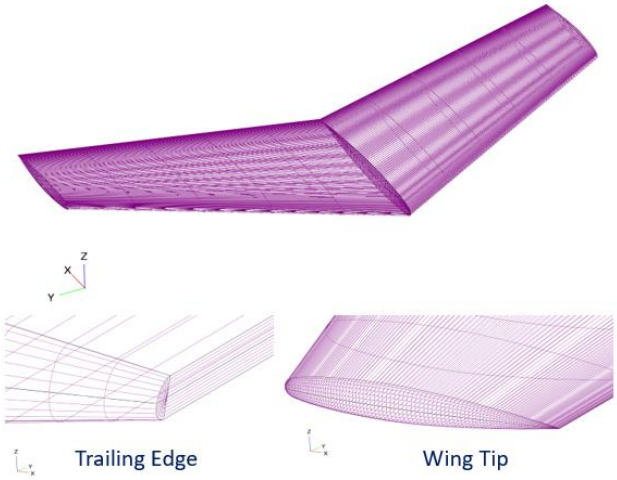

Fig. 2. Representation of parametric model of ONERA M6 wing in OpenVSP

One of the other features of OpenVSP is that it can create customizable surface mesh. By entering the maximum and minimum cell sizes, curve capture coefficient, growth ratio and gap tolerance values suitable for the created parametric model, an unstructured surface mesh can be created. In this study, OpenVSP has been used as the surface mesh generator too since the provided options to generated the required surface meshes were sufficient for the current work. Because it is more customizable and more robust. An example of a generated surface mesh can be visualized in Fig. 3.

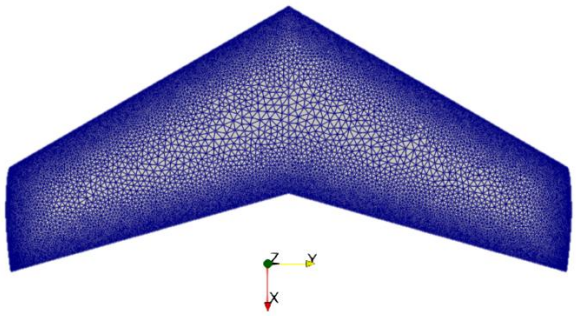

Fig. 3. Top view of surface mesh of ONERA M6 wing

B. *Step-2 (Generating Volume Mesh with SUMO & TetGen)*

SUMO can automatically generate surface and volume unstructured meshes which are to be used for Euler CFD analyses via TetGen. Compared to Delaunay methods, it provides better mesh quality for curved surfaces such as thin, swept delta wings [16]. Also, it triangulates the elements form surface meshes more easily, at least when enough elements are used. Based on surface meshes which have been created by OpenVSP, unstructured volume meshes are created by TetGen to fill the space between the ONERA M6 wing and the far field. Results are exportable as an SU2 mesh file which can be converted to OpenFOAM mesh format using an in-house script. An example of a generated volume mesh is given in Fig. 4.

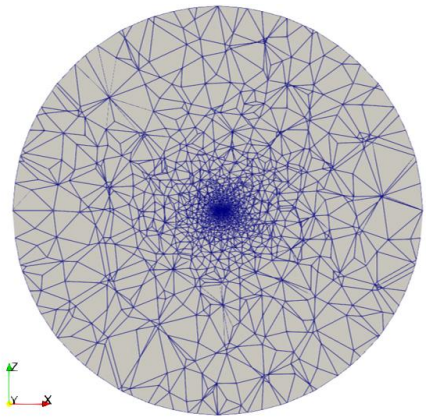

Fig. 4. Volume mesh sliced at Y=0 (Y normal)

C. Step-3 (Numerical Modelling of External Flow over Fixed Wing)

The Navier-Stokes equations describe the behavior of a viscous fluid. When viscous effects are neglected, this simplified form of the governing equations is called the Euler equations. If the Euler equations are formulated in conservative form like in Eq. (1), they allow for accurate representation of shocks, expansion waves and vortices over delta wings [22]. Euler equations which represent the conservation of mass, momentum and energy equations are solved simultaneously at the steady-state for compressible flow using the relevant boundary conditions which are shown in Fig. 5. conservative variables vector W consists in three dimensions of five components given in the Eq. (2). The convective fluxes vector can be written as in Eq. (3). In the Cartesian coordinate system, velocity vector is decomposed in three directions as in Eq. (4).

$$\frac{\partial}{\partial t}\int_{\Omega}\vec{W}d\Omega+\oint_{\partial\Omega}\vec{F}_c dS=\int_{\Omega}\vec{Q}d\Omega \tag{1}$$

$$\vec{W}=\begin{pmatrix}\rho\\ \rho u\\ \rho v\\ \rho w\\ \rho E\end{pmatrix} \tag{2}$$

$$\vec{F}_c=\begin{pmatrix}\rho V\\ \rho uV+n_x p\\ \rho vV+n_y p\\ \rho wV+n_z p\\ \rho HV\end{pmatrix} \tag{3}$$

$$V\equiv\vec{V}.\vec{n}=n_x u+n_y v+n_z w \tag{4}$$

Where t, Ω, $\vec{W}$, $\vec{F}_c$, S, $\vec{Q}$, ρ, u, v, w, $\vec{V}$, E, p, H, $\vec{n}$, denotes, time, control volume, conservative variables, vector of convective fluxes, surface surrounding the control volume, source term, density, x-component of velocity, y-component velocity, z-component velocity, solid body velocity vector, total energy per unit mass, pressure flux vector, total specific enthalpy, unit normal vector, respectively.

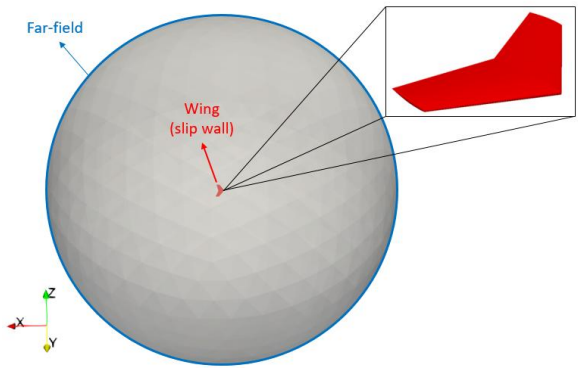

Fig. 5. Boundary conditions of the computational domain

The computational domain has been modelled as a spherical shape of 30 times greater than the chord length of the wing [21]. The standard compressible OpenFOAM solvers have stability and accuracy issues [23]. ASO requires highly stable solver, for this reason, analyses have been carried out using the High-Speed Aerodynamic (HiSA) [24] solver for this regime. In the discretization of the convective term, the second-order AUSM^{+}-up scheme [25] has been used, while for the diffusive terms, a second order Gauss linear corrected numerical scheme has been utilized [26].

In this study, mesh independency studies have been carried out using 3 different Euler meshes. Fine mesh consists of approximately 4 million cells and has 5.5 times more cells than the coarse mesh. The difference in drag and lift coefficients between fine mesh and medium mesh is less than 2% as shown in Table II. The obtained coefficient of pressure (C_P) is compared with experimental results in Fig. 6. [20]. In the latter table, the global force coefficients are compared with another study in the literature [21]. The results are shown on Table II. As one can see, there is discrepancy of less than 6% between coarse and fine mesh in drag coefficient C_D. In addition to the small C_D difference between fine and coarse meshes, the coarse mesh configuration is used in the optimization cycle to reduce the computational cost.

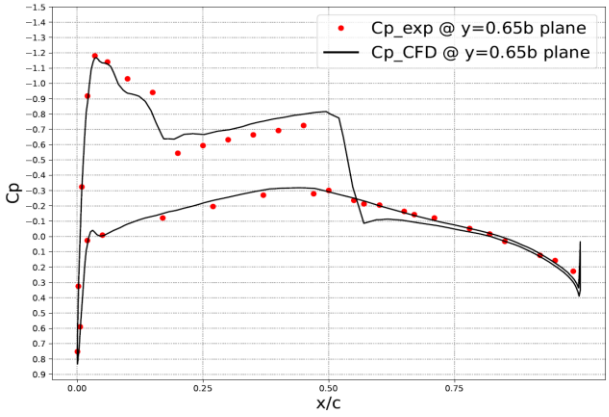

Fig. 6. Coefficient of pressure results at y=0.65b section of the wing

TABLE II: COMPARISON OF FORCE COEFFICIENTS WITH YAMAZAKI ET AL. [21]

	Yamazaki et al. [21]	Coarse Mesh	Medium Mesh	Fine Mesh
C_L	0.28374	0.28032	0.28550	0.28535
C_D	0.01798	0.01906	0.01834	0.01807
C_L % Difference	-	-1.21	0.62	0.57
C_D % Difference	-	5.97	1.99	0.49

D. Step-4 (Optimization with DAKOTA)

In the optimization process, it is aimed to maximize or minimize the single object function based on the constraints determined according to the design parameters. The lift coefficients (C_L) and drag coefficients (C_D) have been calculated by using Eq. (5) and (6), respectively. The object function is determined as the lift to drag ratio and the object function is obtained as a result of CFD analysis at each cycle.

$$C_L = \frac{F_L}{\frac{1}{2}\rho_\infty S_w {u_\infty}^2} \tag{5}$$

$$C_D = \frac{F_D}{\frac{1}{2}\rho_\infty S_w {u_\infty}^2} \tag{6}$$

where $\vec{F}$, F_L , F_D , ρ_∞, u_∞ ,, S_w is total force, lift force, drag force, freestream density, freestream velocity, surface area of the wing, respectively. Aerodynamic forces are calculated in OpenFOAM by integrating the pressure values on the wing surface as in Eq. (7). After calculating the aerodynamic force, lift and drag forces can be found as given in Eq. (8) and (9).

$$\vec{F} = \int_{wing} (\tau + p\vec{I}) \cdot d\vec{S} = \sum_{i=0}^{nf\,(wing)} (\tau_i + p_i \vec{I}) \cdot \vec{S}_i \tag{7}$$

$$F_L = \vec{F} \cdot \vec{n}_{lift} \tag{8}$$

$$F_D = \vec{F} \cdot \vec{n}_{drag} \tag{9}$$

where τ, nf, $\vec{I}$, $\vec{n}_{lift}$, $\vec{n}_{drag}$ is viscous stress tensor, surface elements of the wing, unit vector, direction of lift, direction of drag, respectively.

The optimization process was carried out using the open source based optimization solver DAKOTA where objective function is defined as C_L over C_D. There are both gradient-based and gradient-free optimization algorithms in DAKOTA. Even if gradient-based optimization algorithms work efficiently, there is no certainty to find the global minimum, and it is computationally expensive to calculate gradients at each iteration. In addition, serious effort is required to implement gradient-based optimization algorithms in the flow solver. Gradient-free optimization algorithms can work more efficiently when trying to find the global minimum or maximum value of the object function for a problem with low design parameters.

In the current work, the ONERA M6 wing at the transonic regime was optimized in transonic regime using gradient-free single objective genetic algorithm for 5 different design parameters. Therefore, it would be more advantageous to use gradient-free algorithms. The margin of the design parameters is given in Fig. 7. DAKOTA has been used as black-box in this study. Detailed information about the optimization tool and optimization algorithms is given in [19].

Single Objective Genetic Algorithm
(Gradient free optimization)

Constraints

$1.71 < \text{Aspect Ratio} < 2.09$
$27 < \text{Sweep} < 33$
$0.506 < \text{Taper ratio} < 0.618$
$0.506 < \text{Tip chord} < 0.618$
$-10° < \text{Twist} < 10°$

Fig. 7. Margin of design variables

III. RESULTS AND DISCUSSION

As shown in Fig. 8, it shows the change of the object function in each optimization cycle. It can be clearly seen in Fig. 8 that the object function improves as the number of evaluations increases. This loop can be run further, but the total number of evaluations is limited to 200 for this run. This is because enough relative improvement in object function has been achieved over 200 cycles.

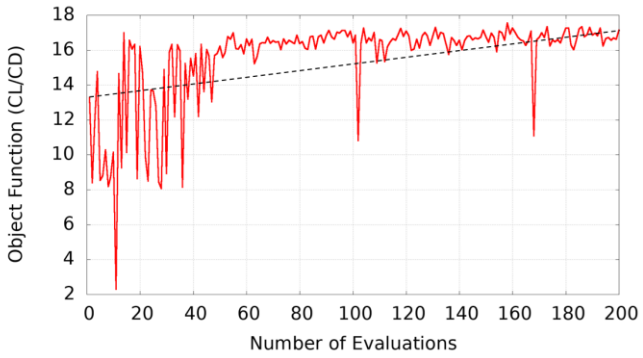

Fig. 8. The object function (C_L/C_D) versus number of evaluations

As a result of 200 evaluations, the object function has been relatively maximized by approximately 17.92%, the results are presented in Table III. The total mesh generation time for the new parametric model in each cycle has been completed in an average of 30 seconds, and the steady-state CFD analysis (1000 iterations to convergence) has been completed in an average of 240 seconds using 160 cores. In total, one cycle is completed in approximately an average of 5 minutes.

TABLE III: THE RESULT OF THE OPTIMIZATION CYCLE IN CURRENT STUDY

Object Function	Before Optimization	After Optimization	Relative Improvement (%)
C_L/C_D	14.707	17.342	17.92

The differences between the initial wing geometry and the optimized wing geometry are shown in Fig. 9. It is clearly seen in Fig. 9 that while the aspect ratio, sweep and taper ratio parameters have been increased, tip chord and twist parameters have been decreased when compared to initial geometry. The design parameters for the optimized and initial wing geometries are presented in Table IV. The obtained pressure coefficient contours for the initial and optimized wing surfaces are plotted in Fig. 10. It can be noted in Fig. 10 that the strength of the shock (i.e. in the blue region on the leading edge) on the optimized geometry is weaker than one on the initial geometry. For this reason, although lift coefficient is slightly decreased, drag coefficient is approximately halved compared to initial geometry. The lift to drag ratio has been improved since the shock strength is less on the optimized geometry.

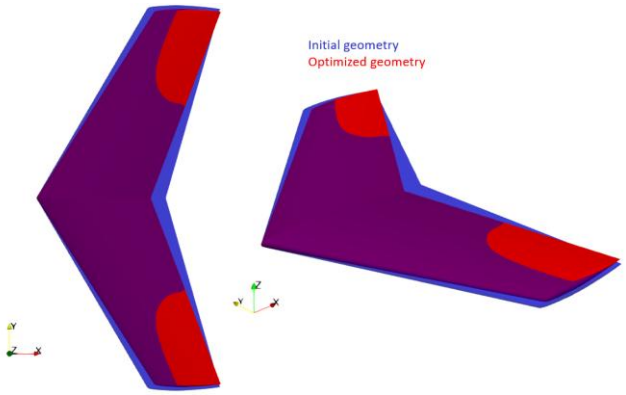

Fig. 9. Initial and optimized wing geometries at different perspectives

TABLE IV: COMPARISON OF DESIGN VARIABLES FOR INITIAL AND OPTIMIZED ONERA M6 WING

Design Variables	Initial Geometry	Optimized Geometry
Aspect Ratio	1.90	2.0769
Sweep	30	31.901
Taper Ratio	0.5622	0.5896
Tip chord (m)	0.5622	0.5210
Twist (°)	0	-1.955

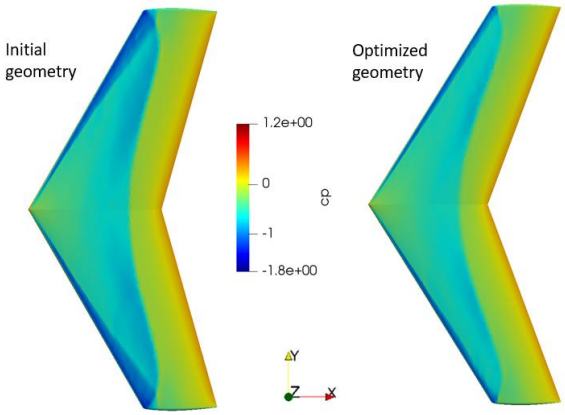

Fig. 10. The pressure coefficient distribution on the wing

IV. CONCLUSIONS

In the present study, a numerical model for the ONERA M6 wing in transonic regime has been created and validated using the experimental results. This numerical model is used in an open source CFD-based ASO workflow to improve the lift to drag ratio. By using the ASO workflow, the lift to drag ratio of the studied wing in the transonic regime has been improved by approximately 17.92%. As a result, the ASO workflow is assumed to be robust enough and works well. This framework can easily be used for aerodynamic applications for other wing geometries and flow conditions without the need for any license.

APPENDIX

The list of symbols is given below in alphabetical order for Latin and Greek separately.

Latin

C_D : drag coefficient [-]

C_L : lift coefficient [-]

C_P : pressure coefficient $(p-p_\infty)/(0.5\rho_\infty|u_\infty|^2)$ [-]

E : total energy per unit mass [J/kg]

$\vec{F}$: total force vector [N]

$\vec{F}_c$: convective fluxes [N]

F_D : drag force [N]

F_L : lift force [N]

H : total specific enthalpy [J/kg]

$\vec{I}$: unit vector [-]

$\vec{n}_{drag}$: drag direction vector

$\vec{n}$: unit vector

n_f : surface elements of the wing [-]

$\vec{n}_{lift}$: lift direction vector

p : pressure flux vector

$\vec{Q}$: source terms vector
S : reference surface area [m²]
S_w : surface area of the wing [m²]
t : time [s]
u : x-component of velocity [m/s]
u_∞ : freestream velocity [m/s]
v : y-component of velocity [m/s]
w : z-component of velocity [m/s]
$\vec{V}$: solid body velocity vector [m/s]
$\vec{W}$: conservative fluid flow variables vector

Greek

ρ : density [m³]
ρ_∞ : freestream density [kg/m³]
τ : viscous stress tensor [N/m²]
Ω : control volume [-]

ACKNOWLEDGMENT

Authors gratefully acknowledge Turkish Aerospace (TA) for providing HPC sources.

REFERENCES

[1] Z. Chen, M. Zhang, Y. Chen, W. Sang, Z. Tan, D. Li and B. Zhang, "Assessment on critical technologies for conceptual design of blended-wing-body civil aircraft," *Chinese Journal of Aeronautics*, vol. 32, pp. 1797-1827, August 2019. https://doi.org/10.1016/j.cja.2019.06.006

[2] Environment Branch of ICAO, "ICAO environmental report: Aviation and climate change," International Civil Aviation Organ, Montreal 2016.

[3] Macintosh, A., & Wallace, L. "International aviation emissions to 2025: Can emissions be stabilised without restricting demand?," *Energy Policy*, vol. 37, pp. 264-273, January 2009. https://doi.org/10.1016/j.enpol.2008.08.029

[4] C. Nickol, and L. Mccullers, "Hybrid Wing Body Configuration System Studies," *47th AIAA Aerospace Sciences Meeting including The New Horizons Forum and Aerospace Exposition*, January 2009. https://doi.org/10.2514/6.2009-931

[5] European Commission Directorate-General for Mobility and Transport, Directorate-General for Research and Innovation, "Flightpath 2050: Europe's vision for aviation," *Publications Office*, June 2011.

[6] A. Mahashabde, P. Wolfe, A. Ashok, C. Dorbian, Q. He, A. Fan, S. Lukachko, A. Mozdzanowska, C. Wollersheim, S. R. H Barrett, M. Locke and I. A. Waitz, "Assessing the environmental impacts of aircraft noise and emissions," *Progress in Aerospace Sciences*, vol. 47 pp. 15-52, January 2011. https://doi.org/10.1016/j.paerosci.2010.04.003

[7] A. Abbas, J. de Vicente and E. Valero, "Aerodynamic technologies to improve aircraft performance," *Aerospace Science and Technology*, vol. 28, pp. 100-132, July 2013. https://doi.org/10.1016/j.ast.2012.10.008

[8] J. Slotnick, A. Khodadoust, J. Alonso, D. Darmofal, W. Gropp, E. Lurie, and D. Mavriplis, "CFD Vision 2030 Study: A Path to Revolutionary Aerosciences," *NASA/CR-2014-218178*, March 2014.

[9] A. Arias-Montaño, C. A. Coello Coello, and E. Mezura-Montes, "Evolutionary Algorithms Applied to Multi-Objective Aerodynamic Shape Optimization," *Computational Optimization, Methods and Algorithms*, vol. 356, pp. 211-240, 2011. https://doi.org/10.1007/978-3-642-20859-1_10

[10] W. Song and A.J. Keane, "Surrogate-based aerodynamic shape optimization of a civil aircraft engine nacelle,". *AIAA Journal*, vol. 45, pp. 2565-2574, October 2007. https://doi.org/10.2514/1.30015

[11] D. López et al., "Framework for the shape optimization of aerodynamic profiles using genetic algorithms," Mathematical Problems in Engineering, vol. 2013, pp. 1-11, October 2013. https://doi.org/10.1155/2013/275091

[12] S. Koziel and L. Leifsson, "Surrogate-based aerodynamic shape optimization by variable-resolution models,". AIAA Journal, vol. 51, pp. 94-106, January 2013. https://doi.org/10.2514/1.J051583

[13] S. Yigit, S. Abuhanieh, and B. Biçer, "An Open-Source Aerodynamic Shape Optimization Application for an Unmanned Aerial Vehicle (UAV) Propeller: An open-source aerodynamic shape optimization application," JAST, vol. 15, no. 2, pp. 1–12, July 2022.

[14] B. Liu, H. Liang, Z.-H. Han and G. Yang, "Surrogate-based aerodynamic shape optimization of a morphing wing considering a wide Mach-number range," Aerospace Science and Technology, vol. 24, p. 107557, May 2022. https://doi.org/10.1016/j.ast.2022.107557

[15] R. A. McDonald and J. R. Gloudemans, "Open Vehicle Sketch Pad: An Open Source Parametric Geometry and Analysis Tool for Conceptual Aircraft Design," AIAA 2022-0004, AIAA SCITECH 2022 Forum, San Diego, CA and Virtual, 3-7 January, 2022. https://doi.org/10.2514/6.2022-0004

[16] M. Tomac and D. Eller, "Towards automated hybrid-prismatic mesh generation," Procedia Engineering, vol. 82, pp. 377–389, 2014. Available: http://www.larosterna.com https://doi.org/10.1016/j.proeng.2014.10.398

[17] Hang Si. "TetGen, a Delaunay-Based Quality Tetrahedral Mesh Generator," ACM Trans. on Mathematical Software, vol. 41, article 11, February 2015. https://doi.org/10.1145/2629697

[18] "OpenFOAM Web Page," [Online] Available: http://openfoam.com

[19] "DAKOTA Web Page," [Online] Available: https://dakota.sandia.gov/

[20] "Turbulence Model Numerical Analysis 3D ONERA M6 Wing Validation Case," [Online] Available: https://turbmodels.larc.nasa.gov/ONERAwingnumerics_val.html

[21] W. Yamazaki, K. Matsushima and K. Nakahashi, "Application of drag decomposition method to CFD computation results," 23rd AIAA Applied Aerodynamics Conference, Toronto, Ontario, Canada, 6-9 June, 2005. https://doi.org/10.2514/6.2005-4723

[22] J. Blazek, "Computational Fluid Dynamics: Principles and Applications," 3rd ed., pp. 5-25, Amsterdam, 2015.

[23] S. Abuhanieh, H.U. Akay and B. Bicer, "A new strategy for solving store separation problems using OpenFOAM," In Proceedings of the Institution of Mechanical Engineers, Part G: Journal of Aerospace Engineering, vol. 236, pp. 3152-3166, April 2022. https://doi.org/10.1177/09544100221080771

[24] "High Speed Aerodynamic (HiSA) solver Web Page," [Online] Available: https://hisa.gitlab.io/

[25] M.-S. Liou, (2006). A sequel to AUSM, Part II: AUSM+-up for all speeds. Journal of Computational Physics, vol. 214, pp. 137-170, May 2006. https://doi.org/10.1016/j.jcp.2005.09.020

[26] "OpenFOAM User Guide Numerical Schemes," [Online] Available: https://www.openfoam.com/documentation/user-guide/6-solving/6.2-numerical-schemes

Bugra Batan received his B.Sc. degrees in Department of Mechanical Engineering from Gazi University, Turkey in 2018. He is still continuing his M.Sc. education at Gazi University. He is working at the Turkish Aerospace Company in the Computational Fluid Mechanics Department as a CFD Engineer. His areas of interest include fluid mechanics, thermodynamics, heat transfer, CFD aerodynamics, and numerical methods.

Saleh Abuhanieh received his B.Sc. degree in Electrical Power Engineering from Yarmouk University Jordan in 2008. He received his M.Sc. degree in Electrical Engineering from KFUPM University, Saudi Arabia in 2012. He received his PhD degree from the Mechanical Engineering Faculty at Atilim University, Turkey in 2022. He is working at the Turkish Aerospace Company in the Computational Fluid Mechanics Department as a Senior CFD Engineer.

Tamer Calisir obtained his B.Sc. in mechanical engineering from Kirikkale University, Turkey, in 2008. He became a research assistant at Gazi University in 2011 and completed his M.Sc. thesis also in 2011. He earned

his PhD degree in 2017 from the same department. He became an assistant professor at Gazi University in 2020. Some of his areas of research interest are electronics cooling, fluid jets, application of numerical methods to heat and mass transfer, as well as problems of fluid mechanics, and similar numerical and experimental research areas.

Sahin Yigit received his B.Sc., M.Sc. degrees in Department of Mechanical Engineering from Karadeniz Technical University, Turkey in 2009 and 2011, respectively. He received his PhD degree in School of Engineering from Newcastle University, United Kingdom in 2018. He worked as post-doctoral researcher in the Department of Aerospace Engineering at Bundeswehr University Munich at Germany between 2018-2020. Currently, he is working in the Computational Fluid Mechanics Department as a Senior CFD Engineer at the Turkish Aerospace Company.